

## Effects of Substrate and Polymer Encapsulation on CO<sub>2</sub> Electroreduction by Immobilized Indium(III) Porphyrin

Birdja, Yuvraj Y.; Vos, Rafaël E.; Wezendonk, Tim A.; Jiang, Lin; Kapteijn, Freek; Koper, Marc T.M.

**DOI**

[10.1021/acscatal.7b03386](https://doi.org/10.1021/acscatal.7b03386)

**Publication date**

2018

**Document Version**

Final published version

**Published in**

ACS Catalysis

**Citation (APA)**

Birdja, Y. Y., Vos, R. E., Wezendonk, T. A., Jiang, L., Kapteijn, F., & Koper, M. T. M. (2018). Effects of Substrate and Polymer Encapsulation on CO<sub>2</sub> Electroreduction by Immobilized Indium(III) Porphyrin. *ACS Catalysis*, 8(5), 4420-4428. <https://doi.org/10.1021/acscatal.7b03386>

**Important note**

To cite this publication, please use the final published version (if applicable). Please check the document version above.

**Copyright**

Other than for strictly personal use, it is not permitted to download, forward or distribute the text or part of it, without the consent of the author(s) and/or copyright holder(s), unless the work is under an open content license such as Creative Commons.

**Takedown policy**

Please contact us and provide details if you believe this document breaches copyrights. We will remove access to the work immediately and investigate your claim.

# Effects of Substrate and Polymer Encapsulation on CO<sub>2</sub> Electroreduction by Immobilized Indium(III) Protoporphyrin

Yuvraj Y. Birdja,<sup>†</sup> Rafaël E. Vos,<sup>†</sup> Tim A. Wezendonk,<sup>‡</sup> Lin Jiang,<sup>†</sup> Freek Kapteijn,<sup>‡</sup> and Marc T. M. Koper<sup>\*†</sup>

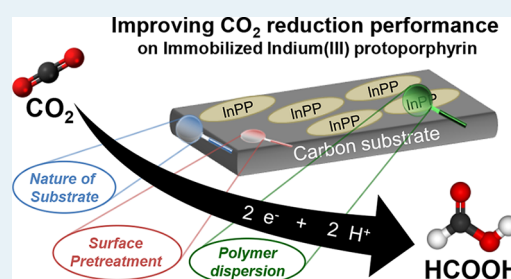
<sup>†</sup>Leiden Institute of Chemistry, Leiden University, P.O. Box 9502, 2300 RA Leiden, The Netherlands

<sup>‡</sup>Catalysis Engineering, Chemical Engineering Department, Delft University of Technology, Van der Maasweg 9, 2629 HZ Delft, The Netherlands

## Supporting Information

**ABSTRACT:** Heterogenization of molecular catalysts for CO<sub>2</sub> electroreduction has attracted significant research activity, due to the combined advantages of homogeneous and heterogeneous catalysts. In this work, we demonstrate the strong influence of the nature of the substrate on the selectivity and reactivity of electrocatalytic CO<sub>2</sub> reduction, as well as on the stability of the studied immobilized indium(III) protoporphyrin IX, for electrosynthesis of formic acid. Additionally, we investigate strategies to improve the CO<sub>2</sub> reduction by tuning the chemical functionality of the substrate surface by means of electrochemical and plasma treatment and by catalyst encapsulation in polymer membranes. We point out several underlying factors that affect the performance of electrocatalytic CO<sub>2</sub> reduction. The insights gained here allow one to optimize heterogenized molecular systems for enhanced CO<sub>2</sub> electroreduction without modification of the catalyst itself.

**KEYWORDS:** CO<sub>2</sub> electroreduction, substrate effect, pretreatment effect, polymer encapsulation, selectivity, activity, stability, immobilization



## INTRODUCTION

The electrocatalytic reduction of carbon dioxide (CO<sub>2</sub>RR) is a potentially efficacious strategy to tackle global energy concerns, particularly to close the carbon cycle and store renewable electrical energy in chemicals or fuels.<sup>1</sup> The latter is highly desired due to the intermittent character of renewable energy production. The last few decades have experienced the discovery and development of various electrocatalysts, which all lead to a diversity of products with different selectivities and activities.<sup>2–4</sup> In addition to heterogeneous CO<sub>2</sub> electrocatalysis using metal, metal alloy, or metal-derived nanostructured electrocatalysts, molecular catalysis of CO<sub>2</sub> has shown interesting properties and has undergone a striking development over the years.<sup>5–8</sup> Molecular catalysts are generally considered to yield high selectivity and activity and can be designed in such a way as to mimic enzymes used in nature to efficiently catalyze specific electrochemical reactions such as hydrogen evolution, water oxidation, carbon dioxide reduction, and oxygen reduction.<sup>6,9</sup> Although their stability and solubility in aqueous electrolytes and their poor robustness are often drawbacks, molecular catalysts are widely used to decipher mechanistic insight due to their well-known molecular structure and efficiency. Hence, many studies have been performed on intrinsic catalyst properties such as the influence of the metal center<sup>10–12</sup> and ligands.<sup>13–17</sup> The focus herein will be on metalloporphyrins, a subgroup of molecular catalysts extensively used for CO<sub>2</sub>RR research.<sup>18,19</sup> In previous work, we

reported that cobalt(II) and indium(III) protoporphyrin IX (InPP) immobilized on pyrolytic graphite exhibit high selectivity toward carbon monoxide and formic acid, respectively.<sup>12,20</sup>

The usually poor solubility of molecular catalysts in aqueous media and need for large amounts of catalyst related to homogeneous molecular catalysts can be overcome by heterogenization. The molecular catalyst is immobilized on a conductive electrode, which we will refer to as “the substrate” in the remainder of this article. An additional advantage of immobilization of the catalyst is the more facile product separation, if the catalyst is utilized in a large-scale industrial process. Carbon materials are often employed as substrates owing to their relatively low cost, robustness, and inert nature toward many (electro)chemical reactions. Examples are pyrolytic graphite, glassy carbon, and more recently boron-doped diamond, carbon nanotubes, and graphene.<sup>21–23</sup> Carbon materials exhibit a rich surface chemistry, and their surface functionalization has been proved to play an important role in their electrochemistry.<sup>24</sup> Studies by Morozan et al. and Rigby et al. have demonstrated the important influence of the carbon support of porphyrins on the selectivity of the oxygen reduction reaction.<sup>22,25</sup> Magdesieva et al. reported on activated carbon

Received: October 4, 2017

Revised: March 27, 2018

Published: April 9, 2018

supports with different pore sizes for CO<sub>2</sub>RR on various porphyrin and phthalocyanine complexes, leading to different selectivities.<sup>26</sup> However, little systematic or comparative work has been performed hitherto, to elucidate the intrinsic influence of the substrate or surface functionalization. The choice of a specific substrate is often solely based on empirical considerations, which is not necessarily the optimal system.

Modification of electrodes started in the early 1980s with several methods such as chemisorption or covalent attachment of species on the electrode surface, encapsulation of species in polymer films, and electropolymerization of monomers directly on the electrode.<sup>27,28</sup> More recently, Yaghi and co-workers developed a covalent organic framework of porphyrin building blocks, which showed promising results for the CO<sub>2</sub>RR.<sup>29</sup> An overview of various catalyst-modified electrodes for CO<sub>2</sub>RR has been given by Sun et al.<sup>30</sup> From heterogeneous electrocatalysis of the CO<sub>2</sub>RR, it is known that the electrode morphology and (sub)surface structure significantly influence the activity and selectivity.<sup>31–33</sup> Moreover, the use of polymers has been shown to enhance CO<sub>2</sub>RR efficiency on cobalt phthalocyanines.<sup>34–36</sup> In the field of heterogenized molecular catalysis of the CO<sub>2</sub>RR, the effects of such substrate modifications are still unexplored. The importance of the chemical functionality on the adsorption and reactivity, as extensively discussed by McCreery,<sup>24</sup> is the inspiration of the idea that substrate modification may affect the reactivity, selectivity, and stability of the CO<sub>2</sub>RR. In a recent review, the importance of so-called secondary phenomena in molecular electrocatalysis has been highlighted.<sup>37</sup> It would be very attractive to be able to tailor the surface chemistry in such a way as to enhance CO<sub>2</sub>RR performance.

In this study we focus on extrinsic properties of the molecular catalyst, particularly related to the immobilization of the molecular catalyst. This work is a step toward a systematic investigation of the chemical functionality of carbon substrates and the chemical environment for heterogenized molecular catalysts. Herein, we study InPP immobilized on different carbon materials, basal-plane pyrolytic graphite (PG), glassy carbon (GC), and boron-doped diamond (BDD), and evince the important role of the substrate, its pretreatment, and the use of polymer membranes for immobilization in the CO<sub>2</sub>RR performance. The current work demonstrates the improvement of CO<sub>2</sub>RR catalysis on heterogenized indium(III) protoporphyrin IX by modifying the substrate, its chemical functionality, and chemical environment of the catalyst. The findings can function as a first step in trying to improve other heterogenized molecular systems as well.

## EXPERIMENTAL SECTION

The electrochemical experiments were carried out with a potentiostat (IviumStat or CompactStat, Ivium Technologies), in a conventional three-electrode cell, where the working electrode (WE) and counter electrode (CE) compartments were separated by a Nafion membrane (Nafion 115). Basal-plane pyrolytic graphite, glassy carbon, and boron-doped diamond disks (5, 5, and 10 mm diameters, respectively) were used as WEs. The counter electrode and reference electrode (RE) were a platinum wire and a reversible hydrogen electrode, respectively. For correct measurements versus the RHE scale, the Luggin capillary and the RHE compartment were filled with CO<sub>2</sub>-saturated electrolyte before CO<sub>2</sub> reduction. The electrolyte is 0.1 M phosphate buffer of pH 9.6 ± 0.1, prepared with K<sub>2</sub>HPO<sub>4</sub>, K<sub>3</sub>PO<sub>4</sub>, and ultrapure water (Millipore Milli-Q gradient A10 system, 18.2 MΩ cm). The

choice for this pH was based on the enhanced HCOOH selectivity observed previously.<sup>12</sup> The reported current densities were always normalized by the geometric surface area of the WE, and in some cases additional normalization by the amount of active species was performed for correct comparison of the activity. The potentials were corrected for ohmic drop by the potentiostat during measurement. Generally, potentiostatic bulk electrolysis was performed at  $E = -1.5$  V vs RHE for 90 min, with manual collection of 100 μL samples at certain times, and analyzed by high-performance liquid chromatography. The reported concentrations of liquid products, or subsequently calculated Faradaic efficiencies (FEs), are an average of three to five independent experiments with freshly prepared electrodes. Additionally, the data points for each experiment were obtained by the average of three injections of the same sample. The dominant contribution of the uncertainty in concentration/FE resulted from the different experiments. Additional experimental details can be found in the Supporting Information.

## RESULTS AND DISCUSSION

**Substrate Effect.** We compare the selectivity and activity for CO<sub>2</sub>RR on InPP immobilized on PG, GC, and BDD substrates. The immobilization procedure and amount of InPP dropcasted per cm<sup>2</sup> were kept the same for all the substrates (details in the Supporting Information). From the Faradaic efficiency toward HCOOH, given in Figure 1a, it is observed

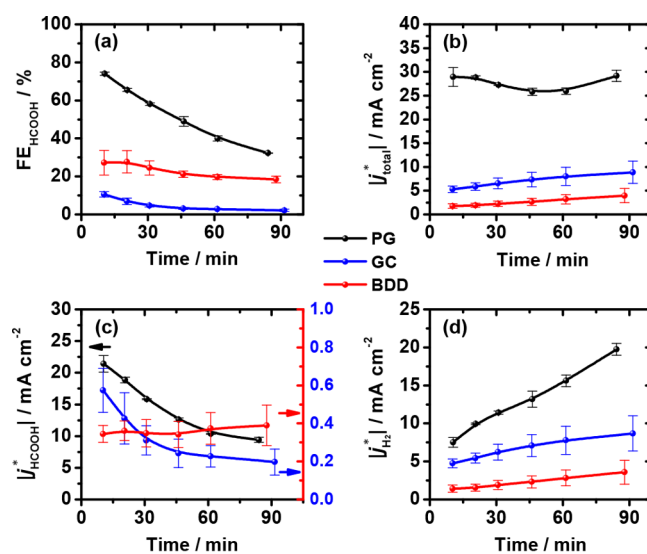


**Figure 1.** (a) Faradaic efficiency toward HCOOH, (b) absolute total current density, (c) absolute partial current density for HCOOH, and (d) absolute partial current density for H<sub>2</sub> during CO<sub>2</sub> reduction on immobilized InPP on different substrates in 0.1 M phosphate buffer of pH 9.6. Lines are given to guide the eye.

that the substrate has a significant influence on the selectivity of the CO<sub>2</sub>RR on immobilized InPP. The PG substrate is the most selective toward HCOOH and the GC substrate the least selective. These effects cannot be ascribed to the activity of the bare substrate, as shown by control experiments in Figure S17a, which show that bare PG, GC, and BDD are not active for the CO<sub>2</sub>RR under our experimental conditions. In Figure 1b–d, the absolute total and partial current densities are shown for the CO<sub>2</sub>RR on the different substrates. For a correct comparison of the activity, the current density was also normalized by the indium content of the substrate (denoted by  $j^*$ ). As will be

discussed in detail later, the electroactive coverages of InPP are not the same for the different substrates. It can be seen that there is a 1 order of magnitude difference in  $j_{\text{total}}^*$  and  $j_{\text{HCOOH}}^*$  on PG in comparison to GC and BDD. Note that this difference is not associated with a difference in electrochemical active surface area (ECSA), as shown in Figure S8a. The fact that GC and BDD both perform worse in comparison to PG indicates that the enhancement in CO<sub>2</sub>RR selectivity and activity cannot be ascribed to the high content of either sp<sup>2</sup> or sp<sup>3</sup> carbon atoms present in GC and BDD, respectively.

The results in Figure 1 are in line with the online mass spectrometry and online HPLC experiments, depicted in parts a and b of Figure 2, respectively, from which we confirm that

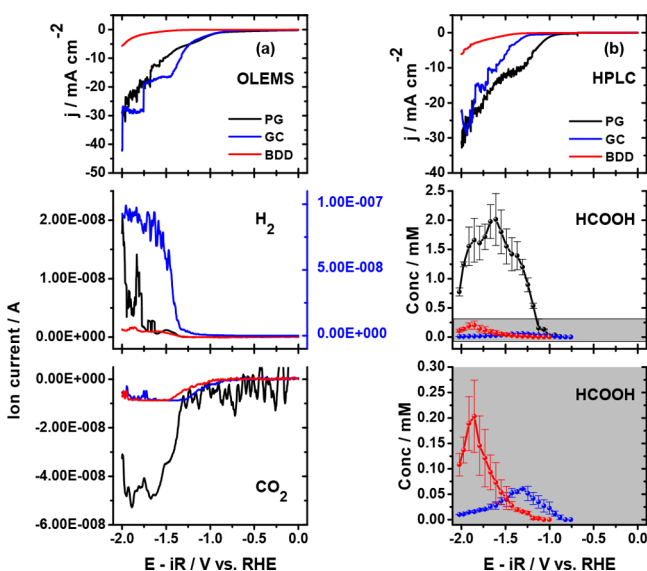


**Figure 2.** (a) Online electrochemical mass spectrometry and (b) online HPLC during CO<sub>2</sub> reduction on immobilized InPP on different substrates in 0.1 M phosphate buffer of pH 9.6.

significantly more H<sub>2</sub> is produced on InPP-GC and significantly more HCOOH on InPP-PG. The CO<sub>2</sub> consumption on InPP-PG is also much higher in comparison to the other substrates, in agreement with higher  $j_{\text{total}}^*$  and the higher HCOOH production rate observed on PG in comparison to the other substrates. Although it is difficult to quantify, the onset potential for H<sub>2</sub> and HCOOH on InPP-BDD is at a more negative potential in comparison to PG and GC, which is a general characteristic of BDD. Moreover, in Figure 2b we can observe differences in the peak potentials of HCOOH formation between the different substrates, which is related to the competition of the hydrogen evolution reaction (HER).

In addition to a change in selectivity and activity, there is a clear difference in stability between the substrates, since a slight decrease is observed in  $j_{\text{HCOOH}}^*$  as a function of time on PG and GC, accompanied by an increase in  $j_{\text{H}_2}^*$ . We define the relative FE with respect to the initial value (eq 1) as a measure for the stability of the system. From a graph of this relative FE versus time (Figure 3a), we can compare experiments with different values of FE. A more horizontal trend indicates a higher stability as the FE does not decrease significantly in time.

$$FE_{\text{relative}} = \frac{FE_t}{FE_{\text{initial}}} \times 100\% \quad (1)$$

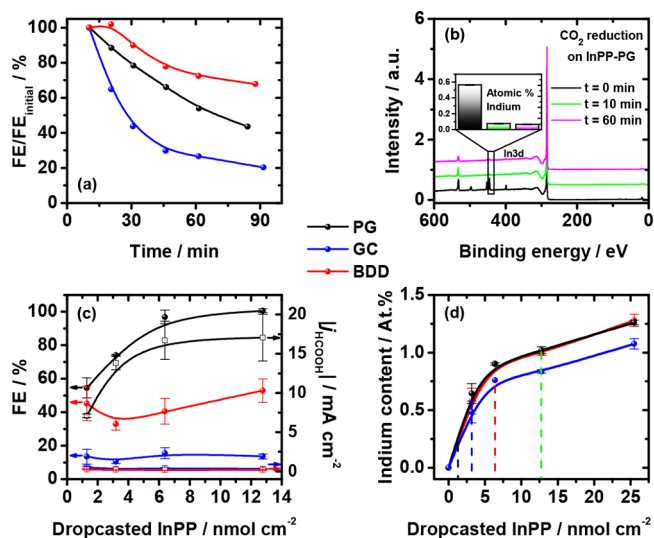


**Figure 3.** (a) Stability of immobilized InPP on different substrates (lines are given to guide the eye), (b) XPS spectra of InPP-PG electrodes before electrolysis and after electrolysis ( $t = 10$  min and  $t = 1$  h) with the indium content (atom %) given in the inset, (c) Faradaic efficiency toward HCOOH (left axis) and partial current density for HCOOH (right axis) as a function of the amount InPP drop-casted on the different substrates (lines given to guide the eye), and (d) indium content of the InPP immobilized on the substrates, as estimated from XPS, as a function of the amount InPP drop-casted (lines given to guide the eye).

The tendency of the FE to decrease with time has been observed before and was associated with the detachment of InPP from the surface or deactivation of the porphyrin.<sup>12</sup> We have performed X-ray photoelectron spectroscopy on InPP-PG before and after electrolysis, as shown in Figure 3b. We observed that the indium content on the electrode, which is a measure of the actual amount of InPP adsorbed on PG, is substantially decreased after 10 min, with a negligible further decrease after 1 h, which is in agreement with the decreasing trend of FE as a function of time. For our work, the charge of redox peaks related to InPP is not an accurate measure to obtain quantitative information about the amount of InPP on the substrate, and we rely on XPS for the quantification of the indium content on the substrate. Additionally, we performed experiments under homogeneous conditions of InPP (Figure S4), in which we do not observe a decrease in selectivity with time. Therefore, we confirm that the destabilization of immobilized indium protoporphyrin is related to detachment from the surface. Moreover, the detachment from the surface takes place in the first 10 min of electrolysis. The adsorption of the porphyrin on the substrate is through noncovalent  $\pi$ - $\pi$  interactions,<sup>30,38,39</sup> which is believed to be important for enhanced CO<sub>2</sub>RR performance and strongly dependent on the carbon substrate.

We believe that the substrate morphology plays an important role, as evidenced by the higher CO<sub>2</sub> consumption observed with OLEMS, which can be explained by efficient mass transport effects due to the more porous structure of PG in comparison to GC or BDD (Figure S8a), which may also suppress the HER. These observations are similar to mass transport effects recently reported for heterogeneous electrocatalysts, showing that the mesostructure can affect the selectivity and activity of the CO<sub>2</sub>RR.<sup>40,41</sup> Additionally, a typical characteristic of GC is its poor permeability for gases,

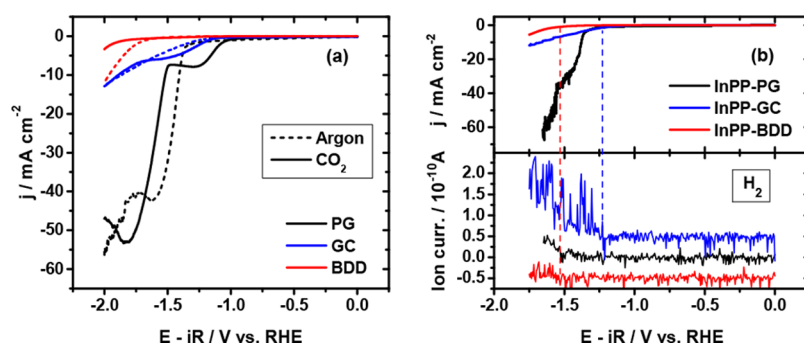


**Figure 4.** (a) Linear sweep voltammetry on immobilized InPP on different substrates in 0.1 M phosphate buffer of pH 9.6 under argon and CO<sub>2</sub> atmospheres (scan rate 20 mV s<sup>-1</sup>) and (b) Online electrochemical mass spectrometry measurement of hydrogen evolution on InPP immobilized on different substrates.

which likely affects the mass transport.<sup>42</sup> X-ray diffractometry and Raman spectroscopy of our substrates (Figures S9a and S10) indicate typical characteristics in agreement with the literature. PG and BDD exhibit sharp XRD peaks, and GC exhibits weak and broad peaks, indicating a high degree of crystallinity for PG and BDD and a somewhat amorphous structure for GC.<sup>43</sup> The Raman spectra indicate the characteristic D and G bands for sp<sup>2</sup> carbons in PG and a specific peak associated with sp<sup>3</sup> carbon in BDD. The Raman bands for GC are weaker and less sharp, which indicate disorder of the graphite lattice for GC.<sup>44,45</sup> The low activity and selectivity on GC may be associated with its poor crystallinity, as a high crystallinity implies enhanced charge transport, as observed in covalent organic frameworks.<sup>29,46</sup> Recently, crystallinity has been shown to play an important role in the selectivity of CO<sub>2</sub>RR on copper phthalocyanine catalysts.<sup>47</sup> However, high crystallinity alone is not sufficient for improved CO<sub>2</sub>RR catalysis, on the basis of the significant differences in CO<sub>2</sub>RR performance between PG and BDD, which are both highly crystalline.

Apart from the substrate morphology and surface structure, a plausible explanation for the enhanced selectivity and activity on PG may be related to a difference in the effective amount of the porphyrin on the three substrates. As can be seen in Figure 3c, a difference in the amount of immobilized InPP on the substrate leads to a difference in activity and selectivity (details of the corresponding experiments are provided in Figures S1–S3). In the case of PG this concentration effect is more pronounced and in the case of GC is almost completely absent, which can be interpreted as a “InPP saturation limit” that is reached earlier for GC in comparison with PG. In other words, the PG substrate can accommodate more catalyst in comparison to GC and BDD. These conclusions are in agreement with quantitative information obtained from XPS spectra of InPP immobilized on the different substrates (Figure S12). We also varied the amount of InPP drop-casted on the different substrates and plotted the indium content as estimated by XPS vs the amount drop-casted in Figure 3d. The vertical dashed lines indicate the InPP amounts used for the qualitative study shown in Figure 3c and Figures S1–S3. It can be seen that the indium content is the highest for PG and the lowest for GC, which is in agreement with our conclusion that a PG substrate can accommodate more catalyst in comparison to GC. Furthermore, we used the indium content of InPP immobilized on different substrates (0.65, 0.49, and 0.58 atom % In on PG, GC, and BDD, respectively) to normalize the activity to the real amount of adsorbed InPP (Figure 1b–d). It

is noteworthy that we assumed that each immobilized InPP molecule contributes to the electrocatalytic activity, and since the difference in indium content between the substrates is small (Figure 3d), we obtain a reasonably accurate comparison of the activities between the substrates.

Another cause of the improved CO<sub>2</sub>RR selectivity may be a difference in HER activity between the substrates instead of solely an intrinsic substrate effect specifically related to the CO<sub>2</sub>RR. In Figure 4a, a comparison between the substrates for the HER and CO<sub>2</sub>RR is shown. The high overpotential for the HER on the BDD substrate does not favor the CO<sub>2</sub>RR, since the CO<sub>2</sub>RR onset potential is shifted toward more negative potentials, and the current is suppressed on InPP-BDD with CO<sub>2</sub> in solution. The HPLC results (Figure 2b) confirm the formation of HCOOH at more negative potentials on BDD in comparison to GC and PG. Under argon, where only hydrogen evolution takes place, the current density on InPP-GC is smaller in comparison to InPP-PG. However, as shown by OLEMS measurements in Figure 4b, more H<sub>2</sub> is produced on GC. Moreover, in the presence of CO<sub>2</sub>, the onset potential is shifted positively for InPP-PG but is almost unchanged for InPP-GC, which indicates a more efficient catalysis of CO<sub>2</sub>RR on PG with respect to GC, in agreement with the online experiments in Figure 2. Consequently, the GC substrate is more active toward the HER in comparison to PG. These results indicate that the competition between CO<sub>2</sub>RR and HER strongly depends on the nature of the substrate, which in turn affects HCOOH selectivity.

In order to increase the impact and generality of our findings, we studied the substrate effect on protoporphyrins with Rh and Sn metal centers, which previously were found to produce HCOOH.<sup>12</sup> Although the HCOOH selectivity for these porphyrins is much lower than for InPP (which is an intrinsic catalytic effect), a trend can be observed for the different substrates similar to that found for InPP (Figure S5). Pyrolytic graphite substrate leads to the highest FE, while the glassy-carbon substrate is the least selective toward HCOOH.

The above results demonstrate the important influence of the substrate, which is believed to be the result of an interplay of several factors influencing the selectivity and reactivity of CO<sub>2</sub>RR, such as morphology/mesostructure (and thereby optimized mass transport effects), crystallinity, electrostatic interaction with the molecular catalyst, and activity for the HER.

**Effect of Substrate Pretreatment.** In addition to the nature of the substrate, modification or treatment of the substrate surface offers a means to influence the CO<sub>2</sub> selectivity,

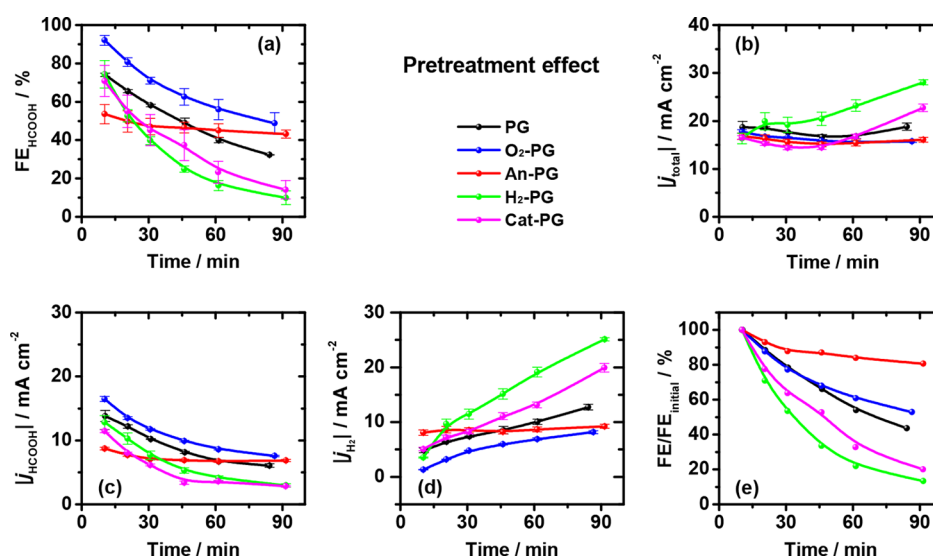


**Figure 5.** (a) Faradaic efficiency toward HCOOH, (b) absolute total current density, (c) absolute partial current density for HCOOH, (d) absolute partial current density for H<sub>2</sub>, and (e) stability during CO<sub>2</sub> reduction on immobilized InPP on different pretreated PG substrates. Electrolyte: 0.1 M phosphate buffer with pH 9.6. Lines are given to guide the eye.

reactivity, and stability. We investigated the influence of a cathodic and anodic electrochemical pretreatment (“Cat-PG” and “An-PG”) and a H<sub>2</sub> and O<sub>2</sub> plasma treatment (“H<sub>2</sub>-PG” and “O<sub>2</sub>-PG”) of the PG substrate. In Figure 5, it is shown that O<sub>2</sub> plasma treatment increases the FE and  $j_{\text{HCOOH}}$  values. These effects can be attributed to a change in chemical functionality as discussed later, instead of an increased surface area as evidenced by similar  $C_{\text{dl}}$  values before and after O<sub>2</sub> plasma treatment (Figure S8b). Since the difference in amount of InPP immobilized on the three substrates is small (Figure 3d), we assume negligible differences in indium content on the various pretreated PG surfaces, and a difference in surface roughness of the pretreated PG electrodes would have a larger influence on the measured current, which is taken into account in our discussion. Furthermore, the exposure time of O<sub>2</sub> plasma seems to play a role, as shown in Figure S6, since a mild O<sub>2</sub> plasma treatment (3 and 6 min exposure) slightly improves the CO<sub>2</sub>RR, while a harsh O<sub>2</sub> plasma treatment (12 min exposure) worsens CO<sub>2</sub>RR performance. In Figure 5e, it is shown that O<sub>2</sub> plasma treatment has negligible influence on the stability. Anodization of PG leads to lower initial FE but improves the stability dramatically. Moreover, both hydrogen treatments, cathodic and H<sub>2</sub> plasma, decrease the selectivity, reactivity, and stability of CO<sub>2</sub>RR significantly. Since H<sub>2</sub>-PG has a lower  $C_{\text{dl}}$  value and thus a smaller surface area (Figure S8b), but a higher  $j_{\text{total}}$  value, the observed changes in selectivity and reactivity do not result from a change in surface area of PG after H<sub>2</sub> plasma treatment.

The observed differences for the investigated pretreated PG substrates highlight the role of oxygenated and hydrogenated functional groups of the substrate’s surface on the immobilization of InPP and subsequently on the CO<sub>2</sub>RR. Our results imply that hydrogen functional groups on the PG surface strongly decrease CO<sub>2</sub>RR selectivity, reactivity and stability and oxygen functionalities increase CO<sub>2</sub>RR performance. H<sub>2</sub> plasma consists of a large amount of H atoms, which react with surface oxides, leading to C–H bonds and a decreased O/C ratio on the surface.<sup>24,48</sup> The chemisorbed hydrogen on the surface promotes the HER with respect to the CO<sub>2</sub>RR, which is reflected in a decrease in FE and  $j_{\text{HCOOH}}$  and increase in  $j_{\text{H}_2}$ . On

the other hand, O<sub>2</sub> plasma treatment increases the amount of oxygen functional groups (e.g., hydroxyl, carbonyl, carboxylate) on the surface, which generally leads to a more polar and hydrophilic surface and stronger adsorbate–substrate interaction. O<sub>2</sub> plasma treated PG shows an improvement in CO<sub>2</sub>RR selectivity. A similar influence of O<sub>2</sub> plasma treatment of the substrate has been reported before for the oxygen reduction reaction.<sup>49</sup>

On anodically treated PG we expected behavior similar to that after O<sub>2</sub> plasma treatment, due to the introduction of oxygenated species, but no improvement in activity or selectivity has been observed. However, a remarkable increase in the stability is observed. On the basis of blank voltammograms of the pretreated PG (Figure S7), there is a significant difference in An-PG in comparison to the untreated and other pretreated PG electrodes. Application of strong anodic pretreatment causes a destruction of the carbon surface and formation of a thick graphite oxide layer, which contains a high amount of anionic sites and interior void volume, leading to high surface area, in agreement with the dramatic increase in  $C_{\text{dl}}$  for An-PG in Figure S8b.<sup>24,50</sup> Complementary information was obtained by X-ray diffractometry, Raman spectroscopy, and X-ray photoelectron spectroscopy. As shown in Figure S9b, the crystalline nature of PG remains intact upon electrochemical pretreatment. However, anodization of PG leads to a significant increase in the Raman peak at  $\sim 1352\text{ cm}^{-1}$  and a slight increase in the D’ peak around  $1620\text{ cm}^{-1}$  (Figure S10b). The peak at  $1352\text{ cm}^{-1}$  is attributed to the presence of graphitic edges, which increases in intensity upon anodic treatment as observed in our spectra, and the peak at  $1620\text{ cm}^{-1}$  indicates delamination of graphitic planes. Formation of graphite oxide increases the strain on the PG lattice, leading to fracturization.<sup>51</sup> In Figure S11 the ratio of the D and G band intensities for the different substrates and pretreated PG is depicted, which clearly shows a high  $I_{\text{D}}/I_{\text{G}}$  ratio in the case of An-PG. Anodization of PG leads to an increase in the edge plane density. Note that GC also exhibits a relatively high  $I_{\text{D}}/I_{\text{G}}$  ratio but showed a poor stability as seen before. Therefore, we believe a high edge plane density in combination with high crystallinity to be the reason for the strongly improved stability. The XPS spectra of the

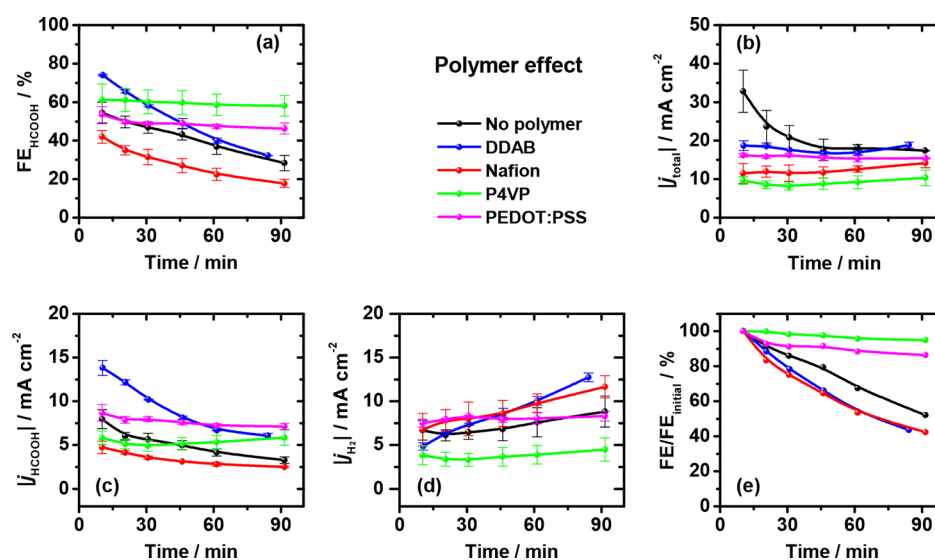


**Figure 6.** (a) Faradaic efficiency toward HCOOH, (b) absolute total current density, (c) absolute partial current density for HCOOH, (d) absolute partial current density for H<sub>2</sub>, and (e) stability during CO<sub>2</sub> reduction on immobilized InPP in different polymer membranes. Electrolyte: 0.1 M phosphate buffer with pH 9.6. Lines are given to guide the eye.

plasma and electrochemically treated pyrolytic graphite electrodes, shown in Figure S13, provide a quantitative basis for our conclusions about chemical functionality on CO<sub>2</sub>RR performance. The oxygen content is significantly higher on An-PG and O<sub>2</sub>-PG in comparison to untreated PG. Moreover, the H<sub>2</sub> plasma and cathodically treated PG exhibit fewer surface oxygenated species in comparison to untreated PG. These results are in agreement with our interpretation of the CO<sub>2</sub>RR results and our Raman spectroscopy experiments.

**Effect of Polymer Encapsulation.** In addition to pretreating the substrate, another strategy aimed at improving CO<sub>2</sub>RR selectivity, reactivity, and stability is incorporation of the porphyrin in polymeric matrices. In this work, we compare the influences of didodecyldimethylammonium bromide (DDAB), Nafion, poly(4-vinylpyridine) (P4VP), and poly(3,4-ethylenedioxythiophene) polystyrenesulfonate (PEDOT:PSS). Details about the immobilization in these polymeric matrices are given in the Supporting Information. The concentration of InPP in the polymer films, and the amount of polymer drop-casted per cm<sup>2</sup> surface were always kept the same. As depicted in Figure 6, interesting differences are observed between the polymer membranes. In comparison with polymer-free InPP (InPP-PG), encapsulation in DDAB, P4VP, and PEDOT:PSS shows enhanced selectivity and activity, whereas Nafion negatively affects the selectivity and activity. From Figure 6d it can be seen that the HER activity with P4VP is drastically decreased. A striking observation in Figure 6e is the enhanced stability when P4VP or PEDOT:PSS is used in comparison to the other polymers. These results underscore the importance of the nature of the polymer, as seen before for a modified bulk silver electrode.<sup>52</sup> Enhanced CO<sub>2</sub>RR performance by P4VP has been reported before for cobalt phthalocyanine, where the authors explain the observed effects by the presence of pyridine residues in the polymer, which influences the coordination to the catalyst.<sup>35,36</sup> Although Nafion-coated catalysts are widely used for various electrocatalytic systems, negative effects of Nafion on the catalytic activity have been observed previously.<sup>53,54</sup>

Differences in polymer-dispersed catalysts are generally associated with the introduction of a hydrophobic environment,

leading to the suppression of the HER.<sup>28,34,55</sup> However, the differences in CO<sub>2</sub>RR performance in our investigation are likely to be explained by the different chemical structures of the polymers (Figure S14), leading to different substrate/adsorbate interactions. As can be seen in the blank CVs in Figure S15, the typical InPP peaks are masked or shifted for Nafion, P4VP, and PEDOT:PSS. Changes in the voltammetric behavior after immobilization of porphyrins in DDAB have been reported before, in which the authors also suggest the possibility of porphyrin dimer formation in DDAB vesicles.<sup>55</sup> The absence of InPP redox peaks in the investigated potential window indicates a change in electrochemical behavior but does not rule out the presence of InPP on the surface, since reasonable amounts of HCOOH are produced. The CV of PEDOT:PSS coated PG shows a much larger double layer, which indicates the strong influence of the polymer on the chemical environment near the electrode surface. The polymers without InPP exhibit reasonable CO<sub>2</sub>RR activity, as can be seen in Figure S17b, where the same trend is observed as for InPP encapsulated in the different polymers. A detailed investigation of the electrocatalytic activity of polymers for CO<sub>2</sub>RR is beyond the aim of this work. Nonetheless, it can be concluded that the observed effects are partially due to the activity of the polymer for CO<sub>2</sub>RR, which is higher with P4VP and PEDOT:PSS. The pyridine group in P4VP and aromatic moieties in PEDOT:PSS are assumed to play an important role in this respect, since Dunwell et al. very recently reported CO<sub>2</sub>RR toward HCOOH mediated by pyridine.<sup>56</sup> The porphyrin exhibits a planar macrocycle with large  $\pi$  conjugation, which facilitates electrostatic interactions with the polymer. We believe that the increased stability is a result of the presence of aromatic building blocks in P4VP and PEDOT:PSS, which facilitates axial coordination to the indium metal center by electron donation. This effect is known for pyridine or imidazole ligands which are used for (covalently) anchoring catalysts to electrodes and are found to stabilize the coordination of CO<sub>2</sub>.<sup>34</sup> This interaction is absent in the case of Nafion and DDAB, leading to a inferior stability in comparison to the polymer-free InPP, P4VP, and PEDOT:PSS. DDAB shows an increase in selectivity and activity, which is associated with the

suppression of the HER similarly to previous work.<sup>52</sup> The poor CO<sub>2</sub>RR performance with Nafion is tentatively ascribed to the low mobility of the porphyrin in the polymer and a disordered structure of the Nafion layer.<sup>53,54</sup> We performed electrochemical impedance spectroscopy on the different polymer-dispersed catalysts to investigate the kinetics of electron-transfer processes (Figure S16). As discussed in the Supporting Information, the charge-transfer resistance between the polymer films is in agreement with the observed activity in Figure 6b. We conclude that the nature of the polymer affects the rate of electron transfer during the CO<sub>2</sub>RR rather than mass transport of active species, leading to different activities among the polymer films.

The results in the present work demonstrate that a hydrophobic environment, induced by the polymer membrane in general, does not always lead to suppression of the HER activity and subsequent improvement of CO<sub>2</sub>RR. Additional effects related to the chemical structure, allowing for electrostatic interactions with the porphyrin or activity toward CO<sub>2</sub>RR by the polymer itself, play an important role. Note that the current findings strongly depend on the (molecular) catalyst under study, and one should be careful to generalize the observed polymer effects for other electrocatalytic systems. Nonetheless, we emphasize the possible negative influence of Nafion on CO<sub>2</sub>RR, as Nafion is very often used to immobilize catalysts or as a binder in the preparation of ink-containing nanoparticulate electrocatalysts.

## CONCLUSION

This work has shown the importance of the nature of the substrate for immobilized indium(III) protoporphyrin IX for CO<sub>2</sub>RR toward formic acid. For this particular system, a pyrolytic graphite substrate outperforms glassy carbon and boron-doped diamond in terms of CO<sub>2</sub>RR selectivity and reactivity, while boron-doped diamond shows the best stability. The enhanced activity and selectivity of PG are assigned to a combination of different factors: first, to a more porous surface structure, leading to efficient mass transport, and furthermore, to an optimal interaction between substrate and InPP and a favorably low HER activity.

We have investigated two strategies to improve or alter the selectivity, reactivity, and stability of the CO<sub>2</sub>RR. Pretreatment of the substrate before catalyst immobilization and immobilization in polymeric matrices have been shown to be practical tools to fine-tune CO<sub>2</sub> reduction performance. Hydrogenated functional groups on the surface decrease the selectivity, activity, and stability, while (mild) oxygen functionalization positively influences the CO<sub>2</sub> reduction performance. Anodization of the graphite surface substantially increases the stability, which is believed to be related to the thick graphite oxide layer containing high edge plane density. Both P4VP and PEDOT:PSS increase the stability, which is believed to be due to axial coordination of their aromatic moieties to the indium metal center. DDAB, P4VP, and PEDOT:PSS improve the performance of the CO<sub>2</sub>RR, while Nafion affects the CO<sub>2</sub>RR negatively. These strategies are assumed to be applicable to similar macrocyclic catalysts immobilized on carbon materials.

It should be noted that the CO<sub>2</sub>RR performance is often a tradeoff among selectivity, activity, and stability, each of which can be modified by substrate pretreatment and catalyst encapsulation in polymers. Although complete mechanistic insight into the pretreatment and polymer effects is still

missing, the results obtained here may help to design heterogenized molecular catalytic systems for CO<sub>2</sub> reduction with specifically optimized properties. Other molecular catalysts may behave differently; hence, one should be careful generalizing the results obtained in this study. However, it is very likely that the substrate, its pretreatment, and catalyst dispersion in polymers will have an influence on CO<sub>2</sub>RR performance, and the insight obtained herein may be used as a starting point for further optimization of the system.

## ASSOCIATED CONTENT

### Supporting Information

The Supporting Information is available free of charge on the ACS Publications website at DOI: 10.1021/acscatal.7b03386.

Experimental details, additional experiments for the substrate effect, pretreated PG, and polymer-coated InPP, and characterization of (pretreated) substrates by X-ray diffractometry, Raman spectroscopy, and X-ray photoelectron spectroscopy (PDF)

## AUTHOR INFORMATION

### Corresponding Author

\*M.T.M.K.: e-mail, [m.koper@chem.leidenuniv.nl](mailto:m.koper@chem.leidenuniv.nl); tel, +31 (0) 71 5274250; fax, +31 (0)71 5274451.

### ORCID

Freek Kapteijn: 0000-0003-0575-7953

Marc T. M. Koper: 0000-0001-6777-4594

### Notes

The authors declare no competing financial interest.

## ACKNOWLEDGMENTS

We thank Dr. Grégory F. Schneider for facilitating the instruments to perform the H<sub>2</sub> and O<sub>2</sub> plasma treatment of pyrolytic graphite electrodes.

## REFERENCES

- (1) Whipple, D. T.; Kenis, P. J. A. Prospects of CO<sub>2</sub> Utilization via Direct Heterogeneous Electrochemical Reduction. *J. Phys. Chem. Lett.* **2010**, *1*, 3451–3458.
- (2) Jones, J.-P.; Prakash, G. K. S.; Olah, G. A. Electrochemical CO<sub>2</sub> Reduction: Recent Advances and Current Trends. *Isr. J. Chem.* **2014**, *54*, 1451–1466.
- (3) Durst, J.; Rudnev, A.; Dutta, A.; Fu, Y.; Herranz, J.; Kaliginedi, V.; Kuzume, A.; Permyakova, A. A.; Paratcha, Y.; Broekmann, P.; Schmidt, T. J. Electrochemical CO<sub>2</sub> Reduction - A Critical View on Fundamentals, Materials and Applications. *Chimia* **2015**, *69*, 769–776.
- (4) Kortlever, R.; Shen, J.; Schouten, K. J. P.; Calle-Vallejo, F.; Koper, M. T. M. Catalysts and Reaction Pathways for the Electrochemical Reduction of Carbon Dioxide. *J. Phys. Chem. Lett.* **2015**, *6*, 4073–4082.
- (5) Collin, J. P.; Sauvage, J. P. Electrochemical Reduction of Carbon dioxide Mediated by Molecular Catalysts. *Coord. Chem. Rev.* **1989**, *93*, 245–268.
- (6) Benson, E. E.; Kubiak, C. P.; Sathrum, A. J.; Smieja, J. M. Electrocatalytic and homogeneous approaches to conversion of CO<sub>2</sub> to liquid fuels. *Chem. Soc. Rev.* **2009**, *38*, 89–99.
- (7) Finn, C.; Schnittger, S.; Yellowlees, L. J.; Love, J. B. Molecular approaches to the electrochemical reduction of carbon dioxide. *Chem. Commun.* **2012**, *48*, 1392–1399.
- (8) Bonin, J.; Maurin, A.; Robert, M. Molecular catalysis of the electrochemical and photochemical reduction of CO<sub>2</sub> with Fe and Co metal based complexes. Recent advances. *Coord. Chem. Rev.* **2017**, *334*, 184–198.
- (9) Savéant, J.-M. Molecular Catalysis of Electrochemical Reactions. Mechanistic Aspects. *Chem. Rev.* **2008**, *108*, 2348–2378.



- (10) Furuya, N.; Matsui, K. Electroreduction of carbon dioxide on gas-diffusion electrodes modified by metal phthalocyanines. *J. Electroanal. Chem. Interfacial Electrochem.* **1989**, *271*, 181–191.
- (11) Chen, L.; Guo, Z.; Wei, X.-G.; Gallenkamp, C.; Bonin, J.; Anxolabéhère-Mallart, E.; Lau, K.-C.; Lau, T.-C.; Robert, M. Molecular Catalysis of the Electrochemical and Photochemical Reduction of CO<sub>2</sub> with Earth-Abundant Metal Complexes. Selective Production of CO vs HCOOH by Switching of the Metal Center. *J. Am. Chem. Soc.* **2015**, *137*, 10918–10921.
- (12) Birdja, Y. Y.; Shen, J.; Koper, M. T. M. Influence of the metal center of metalloprotoporphyrins on the electrocatalytic CO<sub>2</sub> reduction to formic acid. *Catal. Today* **2017**, *288*, 37–47.
- (13) Yamazaki, S.; Yamada, Y.; Takeda, S.; Goto, M.; Ioroi, T.; Siroma, Z.; Yasuda, K. Effects of p-substituents on electrochemical CO oxidation by Rh porphyrin-based catalysts. *Phys. Chem. Chem. Phys.* **2010**, *12*, 8968–8976.
- (14) Costentin, C.; Drouet, S.; Robert, M.; Savéant, J.-M. A Local Proton Source Enhances CO<sub>2</sub> Electroreduction to CO by a Molecular Fe Catalyst. *Science* **2012**, *338*, 90–94.
- (15) Lü, A.; Fang, Y.; Zhu, M.; Huang, S.; Ou, Z.; Kadish, K. M. Dioxygen reduction catalyzed by substituted iron tetraphenylporphyrins in acidic media. *J. Porphyrins Phthalocyanines* **2012**, *16*, 310–315.
- (16) Azcarate, I.; Costentin, C.; Robert, M.; Savéant, J.-M. A Study of Through-Space Charge Interaction Substituent Effects in Molecular Catalysis Leading to the Design of the Most Efficient Catalyst of CO<sub>2</sub>-to-CO Electrochemical Conversion. *J. Am. Chem. Soc.* **2016**, *138*, 16639–16644.
- (17) Zahran, Z. N.; Mohamed, E. A.; Naruta, Y. Bio-inspired cofacial Fe porphyrin dimers for efficient electrocatalytic CO<sub>2</sub> to CO conversion: Overpotential tuning by substituents at the porphyrin rings. *Sci. Rep.* **2016**, *6*, 24533–12.
- (18) Inglis, J. L.; MacLean, B. J.; Pryce, M. T.; Vos, J. G. Electrocatalytic pathways towards sustainable fuel production from water and CO<sub>2</sub>. *Coord. Chem. Rev.* **2012**, *256*, 2571–2600.
- (19) Manbeck, G. F.; Fujita, E. A review of iron and cobalt porphyrins, phthalocyanines and related complexes for electrochemical and photochemical reduction of carbon dioxide. *J. Porphyrins Phthalocyanines* **2015**, *19*, 45–64.
- (20) Shen, J.; Kortlever, R.; Kas, R.; Birdja, Y. Y.; Diaz-Morales, O.; Kwon, Y.; Ledezma-Yanez, I.; Schouten, K. J. P.; Mul, G.; Koper, M. T. M. Electrocatalytic reduction of carbon dioxide to carbon monoxide and methane at an immobilized cobalt protoporphyrin. *Nat. Commun.* **2015**, *6*, 8177.
- (21) Yao, S. A.; Ruther, R. E.; Zhang, L.; Franking, R. A.; Hamers, R. J.; Berry, J. F. Covalently modified graphenes in catalysis, electrocatalysis and photoresponsive materials. *J. Am. Chem. Soc.* **2012**, *134*, 15632–15635.
- (22) Morozan, A.; Campidelli, S.; Filoramo, A.; Jusselme, B.; Palacin, S. Catalytic activity of cobalt and iron phthalocyanines or porphyrins supported on different carbon nanotubes towards oxygen reduction reaction. *Carbon* **2011**, *49*, 4839–4847.
- (23) Navalón, S.; Herance, J. R.; Álvaro, M.; García, H. Covalently modified graphenes in catalysis, electrocatalysis and photoresponsive materials. *Chem. - Eur. J.* **2017**, *23*, 15244.
- (24) McCreery, R. L. Advanced Carbon Electrode Materials for Molecular Electrochemistry. *Chem. Rev.* **2008**, *108*, 2646–2687.
- (25) Rigsby, M. L.; Wasylenko, D. J.; Pegis, M. L.; Mayer, J. M. Medium Effects Are as Important as Catalyst Design for Selectivity in Electrocatalytic Oxygen Reduction by Iron-Porphyrin Complexes. *J. Am. Chem. Soc.* **2015**, *137*, 4296–4299.
- (26) Magdesieva, T. V.; Yamamoto, T.; Tryk, D. A.; Fujishima, A. Electrochemical Reduction of CO<sub>2</sub> with Transition Metal Phthalocyanine and Porphyrin Complexes Supported on Activated Carbon Fibers. *J. Electrochem. Soc.* **2002**, *149*, D89–D95.
- (27) Murray, R. W. Chemically Modified Electrodes. *Acc. Chem. Res.* **1980**, *13*, 135–141.
- (28) Murray, R. W.; Ewing, A. G.; Durst, R. A. Chemically Modified Electrodes. Molecular Design for Electroanalysis. *Anal. Chem.* **1987**, *59*, 379a–390a.
- (29) Lin, S.; Diercks, C. S.; Zhang, Y.-B.; Kornienko, N.; Nichols, E. M.; Zhao, Y.; Paris, A. R.; Kim, D.; Yang, P.; Yaghi, O. M.; Chang, C. J. Covalent organic frameworks comprising cobalt porphyrins for catalytic CO<sub>2</sub> reduction in water. *Science* **2015**, *349*, 1208–1213.
- (30) Sun, C.; Gobetto, R.; Nervi, C. Recent advances in catalytic CO<sub>2</sub> reduction by organometal complexes anchored on modified electrodes. *New J. Chem.* **2016**, *40*, 5656–5661.
- (31) Li, C. W.; Kanan, M. W. CO<sub>2</sub> Reduction at Low Overpotential on Cu Electrodes Resulting from the Reduction of Thick Cu<sub>2</sub>O Films. *J. Am. Chem. Soc.* **2012**, *134*, 7231–7234.
- (32) Chen, Y.; Li, C. W.; Kanan, M. W. Aqueous CO<sub>2</sub> Reduction at Very Low Overpotential on Oxide-Derived Au Nanoparticles. *J. Am. Chem. Soc.* **2012**, *134*, 19969–19972.
- (33) Mistry, H.; Varela, A. S.; Bonifacio, C. S.; Zegkinoglou, I.; Sinev, I.; Choi, Y.-W.; Kisslinger, K.; Stach, E. A.; Yang, J. C.; Strasser, P.; Cuenya, B. R. Highly selective plasma-activated copper catalysts for carbon dioxide reduction to ethylene. *Nat. Commun.* **2016**, *7*, 12123.
- (34) Abe, T.; Yoshida, T.; Tokita, S.; Taguchi, F.; Imai, H.; Kaneko, M. Factors affecting selective electrocatalytic CO<sub>2</sub> reduction with cobalt phthalocyanine incorporated in a polyvinylpyridine membrane coated on a graphite electrode. *J. Electroanal. Chem.* **1996**, *412*, 125–132.
- (35) Yoshida, T.; Kamato, K.; Tsukamoto, M.; Iida, T.; Schlettwein, D.; Wöhrle, D.; Kaneko, M. Selective electrocatalysis for CO<sub>2</sub> reduction in the aqueous phase using cobalt phthalocyanine/poly-4-vinylpyridine modified electrodes. *J. Electroanal. Chem.* **1995**, *385*, 209–225.
- (36) Kramer, W. W.; McCrory, C. C. L. Polymer coordination promotes selective CO<sub>2</sub> reduction by cobalt phthalocyanine. *Chem. Sci.* **2016**, *7*, 2506–2515.
- (37) Savéant, J.-M. Molecular Electrochemistry: Recent Trends and Upcoming Challenges. *ChemElectroChem* **2016**, *3*, 1967–1977.
- (38) Fuhrhop, J.-H. Porphyrin Assemblies and Their Scaffolds. *Langmuir* **2014**, *30*, 1–12.
- (39) Maurin, A.; Robert, M. Noncovalent Immobilization of a Molecular Iron-Based Electrocatalyst on Carbon Electrodes for Selective, Efficient CO<sub>2</sub> to CO Conversion in Water. *J. Am. Chem. Soc.* **2016**, *138*, 2492–2495.
- (40) Kas, R.; Hummadi, K. K.; Kortlever, R.; de Wit, P.; Milbrat, A.; Luiten-Olieman, M. W.; Benes, N. E.; Koper, M. T. M.; Mul, G. Three-dimensional porous hollow fibre copper electrodes for efficient and high-rate electrochemical carbon dioxide reduction. *Nat. Commun.* **2016**, *7*, 10748.
- (41) Yoon, Y.; Hall, A. S.; Surendranath, Y. Tuning of Silver Catalyst Mesostructure Promotes Selective Carbon Dioxide Conversion into Fuels. *Angew. Chem., Int. Ed.* **2016**, *55*, 15282–15286.
- (42) Cowlard, F. C.; Lewis, D. C. Vitreous Carbon - A New Form of Carbon. *J. Mater. Sci.* **1967**, *2*, 507–512.
- (43) Hishiyama, Y.; Nakamura, M. X-ray diffraction in oriented carbon films with turbostratic structure. *Carbon* **1995**, *33*, 1399–1403.
- (44) Bowling, R.; Packard, R. T.; McCreery, R. L. Mechanism of Electrochemical Activation of Carbon Electrodes: Role of Graphite Lattice Defects. *Langmuir* **1989**, *5*, 683–688.
- (45) Wang, Y.; Alsmeyer, D. C.; McCreery, R. L. Raman Spectroscopy of Carbon Materials: Structural Basis of Observed Spectra. *Chem. Mater.* **1990**, *2*, 557–563.
- (46) Wan, S.; Gándara, F.; Asano, A.; Furukawa, H.; Saeki, A.; Dey, S. K.; Liao, L.; Ambrogio, M. W.; Botros, Y. Y.; Duan, X.; Seki, S.; Stoddart, J. F.; Yaghi, O. M. Covalent Organic Frameworks with High Charge Carrier Mobility. *Chem. Mater.* **2011**, *23*, 4094–4097.
- (47) Kusama, S.; Saito, T.; Hashiba, H.; Sakai, A.; Yotsushashi, S. Crystalline Copper(II) Phthalocyanine Catalysts for Electrochemical Reduction of Carbon Dioxide in Aqueous Media. *ACS Catal.* **2017**, *7*, 8382–8385.
- (48) Xu, J.; Chen, Q.; Swain, G. M. Anthraquinonedisulfonate Electrochemistry: A Comparison of Glassy Carbon, Hydrogenated Glassy Carbon, Highly Oriented Pyrolytic Graphite, and Diamond Electrodes. *Anal. Chem.* **1998**, *70*, 3146–3154.

(49) Vaik, K.; Schiffrin, D. J.; Tammeveski, K. Electrochemical reduction of oxygen on anodically pre-treated and chemically grafted glassy carbon electrodes in alkaline solutions. *Electrochem. Commun.* **2004**, *6*, 1–5.

(50) Kelly, R. S.; Weiss, D. J.; Chong, S. H.; Kuwana, T. Charge-Selective Electrochemistry at High-Surface-Area Carbon Fibers. *Anal. Chem.* **1999**, *71*, 413–418.

(51) Bowling, R.; Packard, R. T.; McCreery, R. L. Activation of Highly Ordered Pyrolytic Graphite for Heterogeneous Electron Transfer: Relationship between Electrochemical Performance and Carbon Microstructure. *J. Am. Chem. Soc.* **1989**, *111*, 1217–1223.

(52) Quan, F.; Xiong, M.; Jia, F.; Zhang, L. Efficient electroreduction of CO<sub>2</sub> on bulk silver electrode in aqueous solution via the inhibition of hydrogen evolution. *Appl. Surf. Sci.* **2017**, *399*, 48–54.

(53) Buttry, D. A.; Anson, F. C. New Strategies for Electrocatalysis at Polymer-Coated Electrodes. Reduction of Dioxygen by Cobalt Porphyrins Immobilized in Nafion Coatings on Graphite Electrodes. *J. Am. Chem. Soc.* **1984**, *106*, 59–64.

(54) Jarzębińska, A.; Rowiński, P.; Zawisza, I.; Bilewicz, R.; Siegfried, L.; Kaden, T. Modified electrode surfaces for catalytic reduction of carbon dioxide. *Anal. Chim. Acta* **1999**, *396*, 1–12.

(55) de Groot, M.; Koper, M. T. M. Redox transitions of chromium, manganese, iron, cobalt and nickel protoporphyrins in aqueous solution. *Phys. Chem. Chem. Phys.* **2008**, *10*, 1023–1031.

(56) Dunwell, M.; Yan, Y.; Xu, B. In Situ Infrared Spectroscopic Investigations of Pyridine-Mediated CO<sub>2</sub> Reduction on Pt Electrocatalysts. *ACS Catal.* **2017**, *7*, 5410–5419.